scientific reports

Check for updates

OPEN

Listening to heart sounds through the pressure waveform

Alessio Tamborini✉ & Morteza Gharib

Non-invasive diagnostic modalities are integral to cardiovascular care; however, current systems primarily measure peripheral pressure, limiting the breadth of cardiovascular prognostication. We report a novel approach for extracting left side heart sounds using a brachial cuff device. The technique leverages brachial cuff device enhanced signal resolution to capture pressure fluctuations generated by cardiohemic system vibrations, the sound pressure waveform. We analyze left heart catheterization data alongside simultaneous brachial cuff device measurements to correlate sound pressure waveform features with left ventricle (LV) contractility. The extracted sound pressure waveform reveals two prominent oscillatory wave packets, termed WP1 and WP2, originating from cardiac structure vibrations associated with LV contractions and relaxation. We demonstrate that WP1 originates from LV contraction during systolic blood ejection through the aortic valve (AV) and is correlated with LV isovolumetric contraction, clinically measured by LV dPdt-max (Pearson-R = 0.65, $p < 0.001$). Additionally, we show that WP2 comes from LV elongation required for blood flow deceleration at the end of systole, causing AV closure, and is correlated with LV isovolumetric relaxation, measured by LV ndPdt-max (Pearson-R = 0.55, $p < 0.001$). These findings highlight the value of cuff sound pressure waveforms in providing insights about dynamic coupling of the LV-Aorta complex for non-invasive assessment of LV contractility.

Keywords Brachial cuff, Heart sounds, Sound pressure waveform, Left ventricular contractility

The generation of heart sounds is a complex physiological process arising from the energy of cardiac contractions and the interaction of pressure gradients, blood flow, and valvular function[1]. During the cardiac cycle, heart chamber contract to generate positive pressure gradients, open heart valves, and generate forward flow. These forceful contractions bring about abrupt accelerations and decelerations of blood flow that send the entire cardiohemic system (heart and aorta (AO)) into a transient state of vibration. In clinical cardiology, heart sounds are commonly auscultated with a stethoscope as a non-invasive diagnostic indicator for heart valve disease, such as stenosis or regurgitation[2]. However, these sounds encompass a wealth of information about the heart beyond valvular function[3]. The capability of the heart to generate forceful contractions and relaxations, clinically referred to as contractility, is fundamental for the correct functionality of this muscular organ[4]. Inability to generate these pressure differences leads to heart failure. Given the increasing prevalence of left-sided heart failure in the population, there is an unmet need for a non-invasive and rapid method to assess left side heart functions[5,6].

The left ventricle (LV) is responsible for pumping blood out of the heart to the arterial system. At the start of LV systole, the LV undergoes a rapid pressure rise during isovolumetric contraction, which causes the aortic valve (AV) to open forcefully. The energy input for the forceful acceleration of blood into the aorta AO generates transient pressure vibrations referred to as aortic ejection sounds (AES), a component of the first heart sound[7–9]. At the end of systole, the LV undergoes a rapid pressure drop during isovolumetric relaxation, which rapidly decelerates blood flow and causes the AV to close. The rapid change in momentum of flow generates transient cardiac vibrations that are the origin of the second heart sound[9–15]. These cardiac system vibrations produce complex pressure waveforms whose characteristics are dependent on the underlying system properties[9]. These complex vibrational waveforms are composed of lower and higher frequency content[9]. The higher frequency content radiates from the cardiac tissue into the chest wall and can be auscultated with a stethoscope. On the other hand, the lower frequency content, the sound pressure waveform, is embedded and superimposed in the cardiac pressure waveform[9]. Yet, given the significantly smaller relative amplitude of the signal, this information is hidden by the dominant frequencies of the cardiac pressure wave.

The sound pressure waveform has been previously measured in the ascending AO and LV by using invasive catheter methods[7,10]. These studies demonstrated that the pressure vibration amplitudes generated by the LV-AV interactions closely correlate to the rates of pressure change in the LV. It has been reported that increased LV

Department of Medical Engineering, California Institute of Technology, Pasadena, CA, USA. ✉email: atambori@caltech.edu

isovolumetric contraction produces a faster pressure rise and results in AES of greater amplitude[7]. Similarly, the amplitude of the second heart sound has been shown to be directly correlated to the rate of pressure fall during LV isovolumetric relaxation[16–24]. While these studies discovered and characterized this signal, the invasive nature of the catheter limited the applicability of such measurements. In contrast, a non-invasive method capable of measuring the sound pressure waveform could present a valuable tool for assessing LV contractile and relaxation rates. However, it is noteworthy that stethoscopes cannot be a substitute as they are unable to capture the low frequency component of the sound pressure waveform[9,17,25].

This study introduces a cuff-based method to extract the sound pressure waveform for non-invasive assessment of the LV-AV coupling, focusing on evaluating LV contractility. The small amplitude of the sound pressure waveform has only recently become measurable with cuff-based devices thanks to advancements in high-resolution signal acquisition. Using invasive catheter measurements as reference, this study aims to demonstrate that the proposed method can reliably capture the sound pressure waveform non-invasively. First, the high-resolution cuff-based system is used to extract the sound pressure waveform from brachial measurements[26]. The method is then evaluated in a clinical study against simultaneous invasive catheter recordings. Finally, sound pressure waveform features are correlated with LV maximal contraction rate (dPdt-max) and maximal relaxation rate (ndPdt-max), assessing isovolumetric contraction and relaxation strength[4,27].

Results

Study population

The invasive study enrolled 202 subjects who were referred and pre-scheduled for left heart catheterization. Notably, 159 recordings from this population satisfied the device hardware requirements. Following the exclusion criteria, 43 individuals were excluded: 5 for severe atrial fibrillation, 3 for incorrect procedure, and 32 for apparatus malfunction (14 catheter failures, 7 brachial cuff failures, and 11 data acquisition faults), and 3 for abnormal catheter pressure signals (LV pressure always smaller than the AO pressure upon catheter retraction). Algorithmic filtering excluded an additional 10 individuals for low quality recordings in the suprasystolic blood pressure (sSBP) hold. Participant inclusion is summarized in Fig. S1 using a flowchart.

The population (n = 106) was composed of 65% men, the average age was 66 years, and the average BMI was of 29.1. In the study population, 81% reported hypertension, 31% reported diabetes, and 75% reported hyperlipidemia. High prevalence of heart valve disease was present: 23% reported heart valve disease, 6% reported aortic stenosis and 5% reported aortic regurgitation. Table 1 summarizes the main characteristics of the study population.

Variable	Quantity (n = 106)
Clinical characteristics	
Age, (years)	66 ± 9
Men, n (%)	69 (65%)
Weight, (kg)	86.1 ± 18.9
Body mass index, (kg/m^2)	29.1 ± 5.6
Left arm circumference, (cm)	31.8 ± 4.0
White, n (%)	77 (73%)
Comorbidities	
Hypertension, n (%)	86 (81%)
Diabetes, n (%)	33 (31%)
Thyroid, n (%)	17 (16%)
Hyperlipidemia, n (%)	80 (75%)
Smoker, n (%)	18 (17%)
Cardiovascular disease	
Carotid artery disease, n (%)	25 (24%)
Cardiomyopathy, n (%)	12 (11%)
Heart failure, n (%)	19 (18%)
Heart valve disease, n (%)	24 (23%)
Aortic stenosis, n (%)	6 (6%)
Aortic regurgitation, n (%)	5 (5%)
Heart surgery, n (%)	10 (9%)
Left ventricular dysfunction, n (%)	15 (14%)
Myocardial infarction, n (%)	16 (15%)
Peripheral vascular disease, n (%)	20 (19%)
Pacemaker, n (%)	3 (3%)
Stroke, n (%)	2 (2%)

Table 1. Characteristics of study participants. Data in table summarizes the clinical characteristics of the population used in this study; the data is mean ± standard deviation, unless otherwise stated.

Evaluation of sound pressure digital filtering method

The method to extract the sound pressure waveform from the brachial cuff recording, as outlined in Fig. 1, was successfully applied to the sSBP pulse waveform signals from the entire study population (n = 106). The digital filter for sound pressure waveform extraction was optimized for filter type and cutoff frequency (Fig. S2 and Note S1). Optimal signal reconstruction was obtained with a 4th order elliptic high-pass filter with 20 Hz cutoff frequency. These filtering characteristics are used throughout the rest of the study. Future device iterations can integrate in analog format the filter specified for onboard sound pressure waveform measurement.

The cardiac cycle in the extracted sound pressure waveforms consistently featured two distinct oscillatory patterns or wave packets, termed WP1 and WP2, followed by a long quiescent interval. The foot of the cardiac pressure waveform marked the start of the cardiac cycle. Figure 2A shows example segments of sound pressure waveform signals extracted in the sSBP hold from three subjects in the study population. All signals consistently displayed this double peak nature characteristic of the sound pressure waveform as described in the literature.

The cuff sound pressure waveform feature timing in cardiac cycle is illustratively compared with respect to the invasive catheter in the AO location adjusted for wave propagation time (Fig. 2B). The WP1 oscillations occur at the onset of AO systole. The start of the WP1 oscillations coincides with the pressure rise in the AO, which physiologically represents the opening of the AV and the acceleration of blood in the AO. The WP2 oscillations occur between the end of systole and the onset of diastole. The start of the WP2 oscillations is simultaneous to the rapid pressure deflections at the dicrotic notch in the AO pressure signal which physiologically marks the closing of the AV and deceleration of blood flow in the AO.

Signal comparison with stethoscope

Simultaneous stethoscope and brachial cuff sound pressure waveforms in the sSBP hold were captured for five young-healthy individual (n = 5) in a non-invasive study at Caltech. Signals from both the cuff sound pressure and the stethoscope showed waveforms with two peaks followed by a quiescent period (Fig. 3A and B). In the stethoscope signal, the first peak, conventionally denoted as S1, is the closure of atrioventricular valves and the second peak, conventionally denoted as S2, is the closure of semilunar valves.

The timing interval between the peaks in the stethoscope and cuff sound pressure waveform was compared on a beat-to-beat basis. Figure 3C reports a median S1 to WP1 peak time delay of 132 ms, 123 ms, 114 ms, 127 ms, and 150 ms and a median S2 to WP2 peak time delay of 80 ms, 76 ms, 80 ms, 67 ms, and 96 ms for the five subjects in this analysis. In all individuals the S1 to WP1 peak time delay is longer than the S2 to WP2 peak time delay; the average difference between the median time delays is of 49 ± 10 ms for the five subjects. The time delays present between the stethoscope and cuff measurement originates from the difference in wave propagation speed. In cuff measurements, sound pressure waveforms propagate embedded within the cardiovascular pulse waveform at the characteristic speed of the arterial pressure wave, the pulse wave velocity. In stethoscope measurements, the signal travels through the chest cavity at the speed of sound, which is significantly larger than pulse wave velocity[28].

The sound pressure signals were analyzed for instantaneous frequency (IF) around the oscillatory pressure peaks: WP1, WP2, S1, and S2. As reported in Fig. 3D the cuff sound pressure signal had a median WP1 IF of 14.2 Hz, 12.5 Hz, 12.2 Hz, 13.2 Hz, and 12.5 Hz and a median WP2 IF of 14.7 Hz, 13.4 Hz, 13.5 Hz, 11.4 Hz, and 12.8 Hz for the five subjects, respectively. The stethoscope sound pressure signal had a median S1 IF of 28.1 Hz, 25.9 Hz, 18.4 Hz, 31.4 Hz, and 32.4 Hz and a median S2 IF of 31.1 Hz, 33.8 Hz, 27.5 Hz, 32.5 Hz and 29.3 Hz (Fig. 3E). The larger variance in the stethoscope results comes from the measurement sensitivity to device

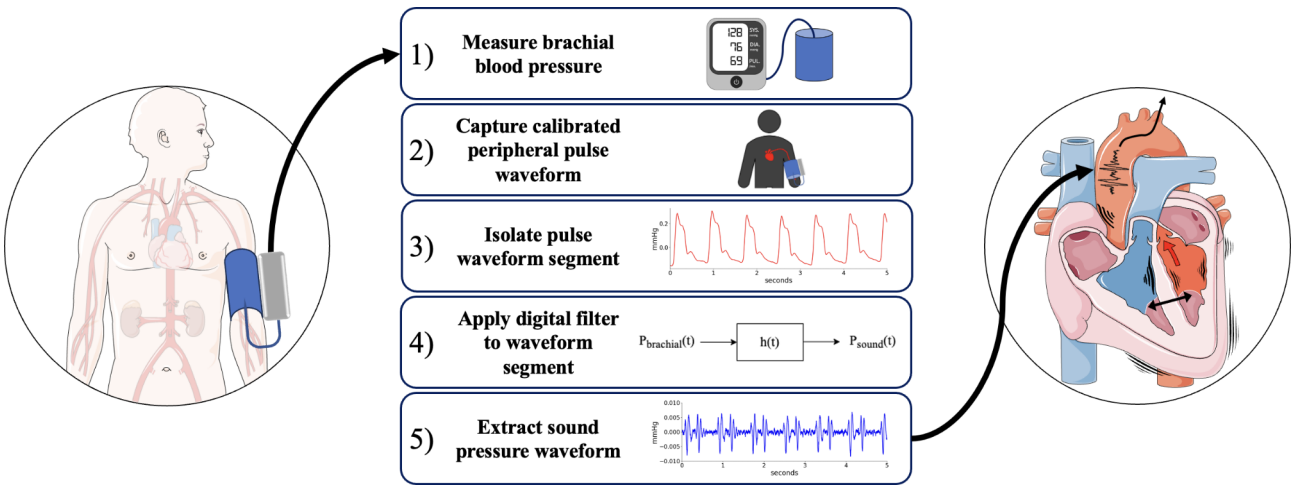

Fig. 1. Method for sound pressure waveform extraction with brachial cuff. Step-by-step method for extracting the cardiovascular sound pressure waveform from a high-resolution brachial cuff device with inflate and hold capabilities. Part of the figure were generated with a modified picture from Servier Medical Art, provided by Servier, licensed under a Creative Commons Attribution 4.0 Unported License.

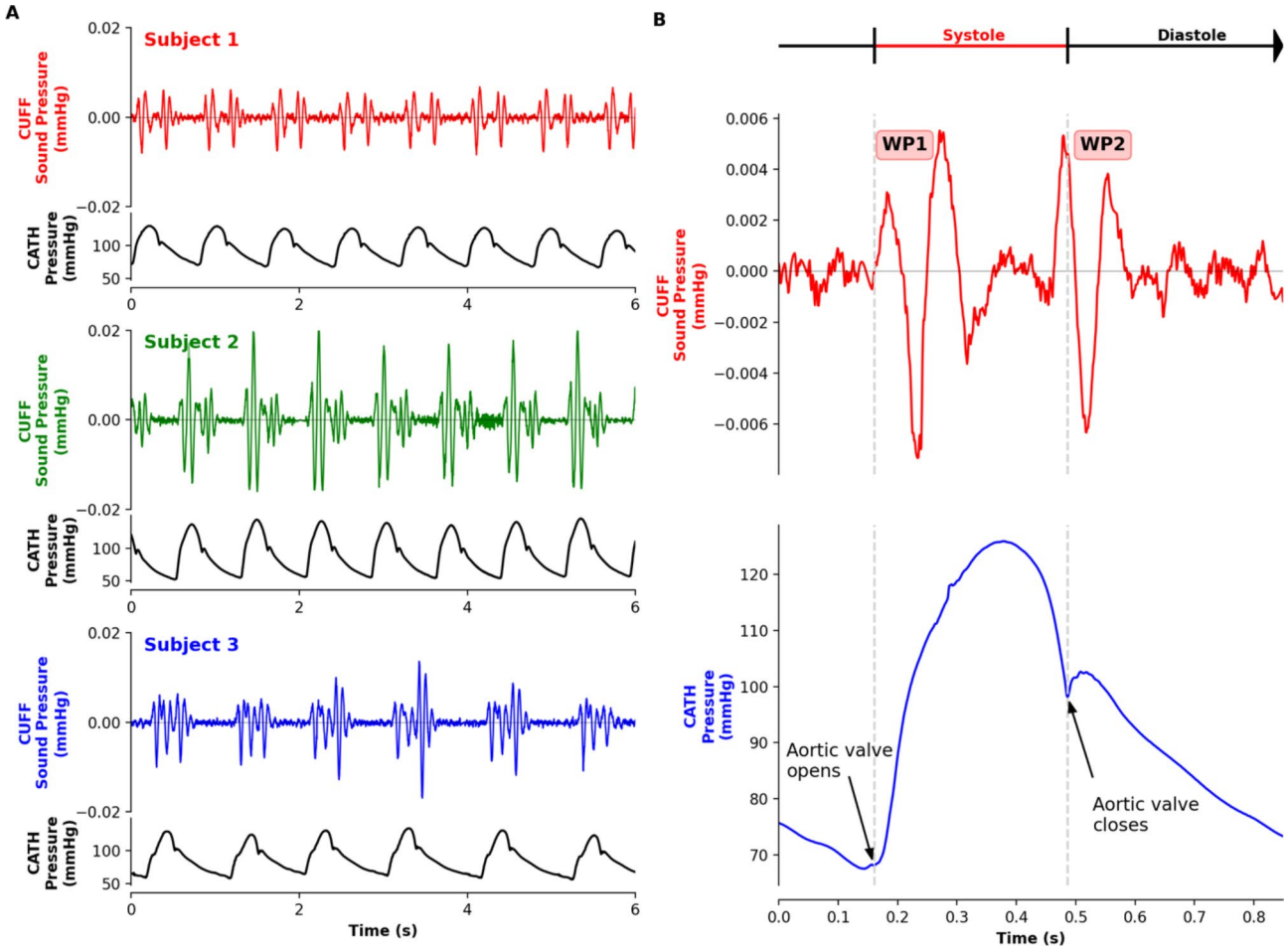

Fig. 2. Sound pressure waveforms from brachial cuff device extracted in a clinical study. (**A**) The three panels of the illustration show the sound pressure waveform extracted in the sSBP hold pressure for different individuals in the study. Catheter pressure signals (black) shown serve as a timing reference for the signals. (**B**) shows the cardiovascular signals timing intervals during a single cardiac cycle inclusive of cuff-based sound pressure waveform (red) and catheter aortic pressure (blue). The sound pressure waveform WP1 and WP2 peaks are labeled for reference. Acoustic pressure waveform has been time shifted using the calculated time delta to correct for wave propagation delay.

placement. These results confirm the cuff sound pressure waveform captures the low frequency component while the stethoscope captures the high frequency component of the cardiac structure vibrations.

Both findings, namely the difference in the time delays and IFs, highlight that WP1 and WP2 in the cuff represent different time intervals and physiological events to the S1 and S2 peaks detected by the stethoscope. The well-established fact that the stethoscope primarily detects the closure of heart valves, coupled with the observation from our study regarding the delayed appearance of the first pressure oscillation in the cuff, strengthens the correlation between the peaks of the cuff-based sound pressure waveform and the opening and closing of the AV[29]. These results further suggest that the stethoscope measurement is not a substitute of the cuff sound pressure waveform information.

Effect of cuff hold pressure on sound pressure waveform morphology

The target pressure in the inflate-and-hold approach varies the pressure-flow relationship in the brachial artery. It has been previously shown that the pulse waveform shows significant morphological changes with hold pressure[26]. The method to extract the sound pressure waveform from the brachial cuff recording was applied at the signals captured in the diastolic blood pressure (DBP), mean arterial pressure (MAP), and sSBP holds. Figure 4 shows overlayed average pressure and extracted sound pressure waveforms for all holds in four subjects from the clinical study. Pulse waveforms between the DBP, MAP, and sSBP hold show significant differences for both morphology and amplitude. On the other hand, sound pressure waveforms displayed compatible features amongst the holds. WP2 oscillations had consistent amplitude, shape, and frequency between all holds. WP1 oscillations had same frequency and shape, yet variable amplitude. Following the WP2 oscillations, all sound pressure waveforms have a flat steady signal.

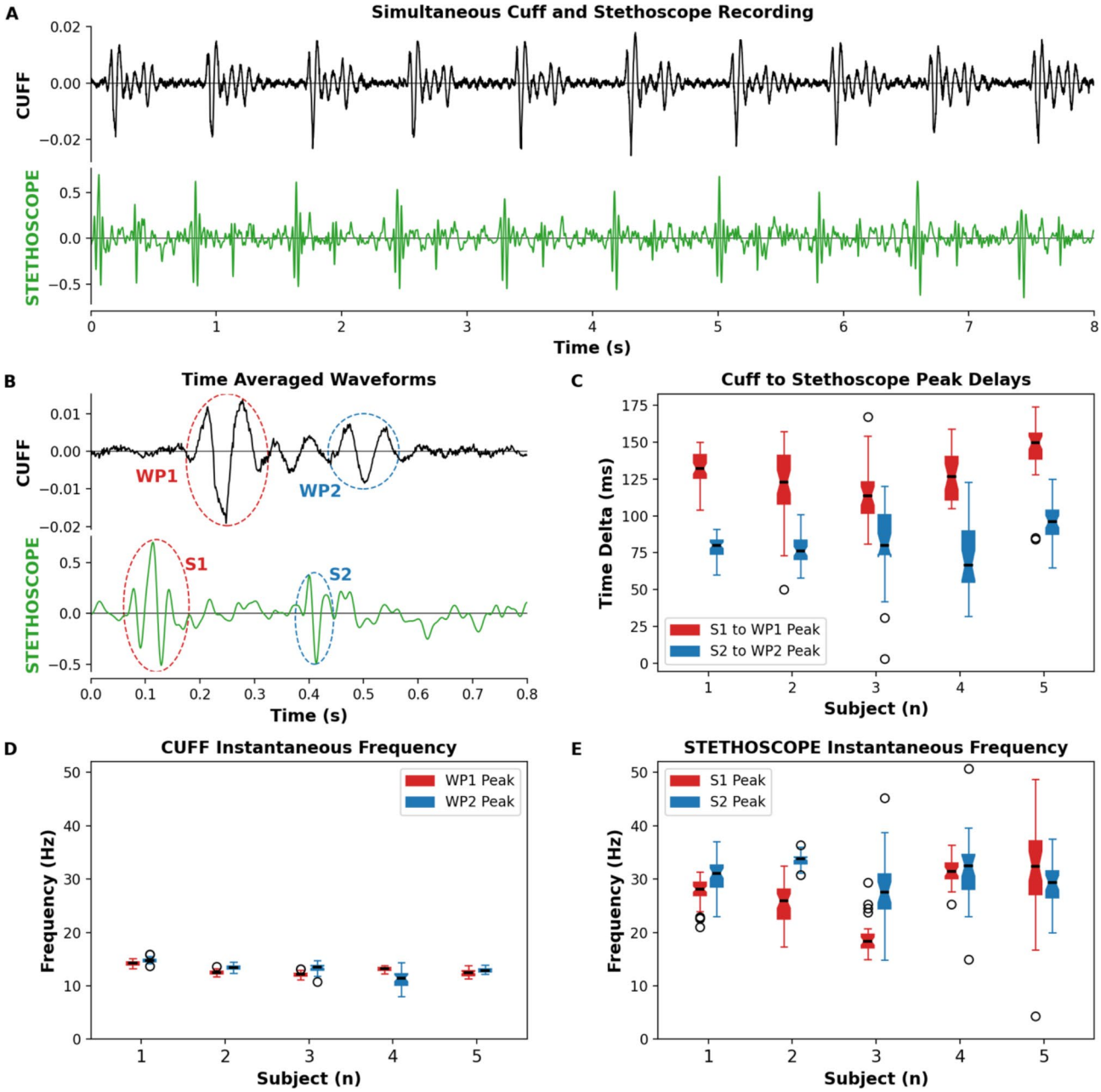

Fig. 3. Sound pressure signal comparison between simultaneous cuff and stethoscope. (**A**) Shows a ten-second segment of simultaneous stethoscope and sSBP hold sound pressure waveforms. (**B**) Shows the average waveform for the cuff and stethoscope highlighting the time shift between the WP1 and WP2 peaks. (**C**) The calculated beat-to-beat time delay between the cuff and stethoscope peaks showing a clear difference between the WP1 and WP2 time deltas. (**D**) shows the Instantaneous Frequency analysis for the WP1 and WP2 cuff sound pressure signal. (**E**) shows the Instantaneous Frequency analysis for the S1 and S2 stethoscope signal.

Beyond flow induced pressure vibrations, the morphology of the sound pressure waveform should be independent of the hold pressure. Indeed, the WP2 oscillations perfectly overlapped in all three holds as no flow is expected at this instance of the cardiac cycle. In contrast, the WP1 oscillations were incrementally affect by local flow. In the presence of flow, arterial restrictions cause arterial wall flutter and local turbulence, known as Korotkoff sounds[30]. Korotkoff sounds are maximal at the MAP hold pressure and the waveform morphologies shown in Fig. 4 align with these expectations. Yet, upon full occlusion of the artery in the sSBP hold, flow is blocked and Korotkoff sounds disappear. Korotkoff sounds can be measured using a stethoscope on the brachial artery under the distal end of the cuff from the heart. In Fig. S3, we show how the sSBP and MAP hold pressure can be combined to extract the Korotkoff sound pressure waveform. The extracted waveform from the brachial cuff closely matches the Korotkoff waveform at the distal end of the brachial cuff measured with the digital stethoscope.

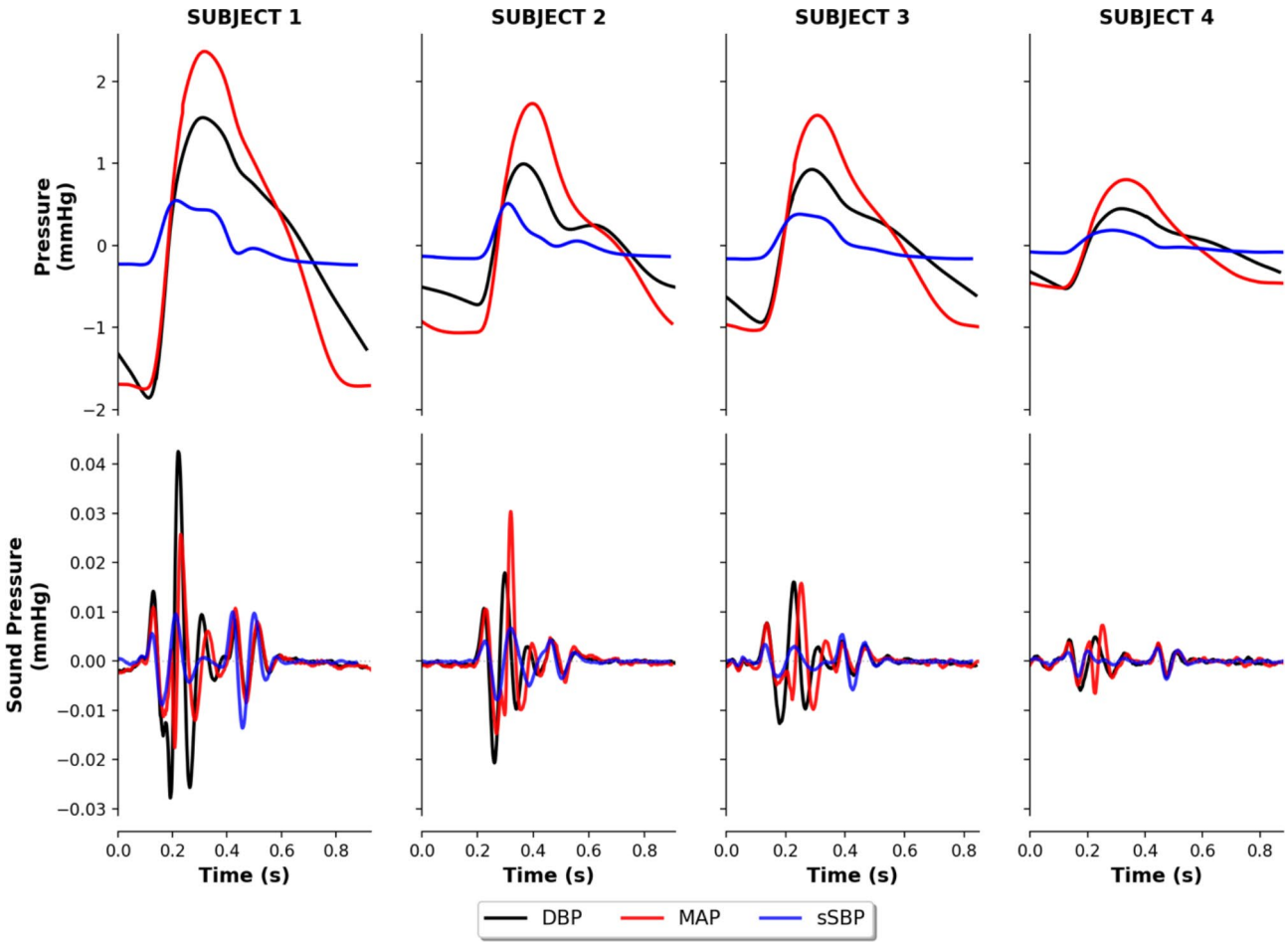

Fig. 4. Effect of the hold pressure on the sound pressure waveform morphology. Comparison between the pulse waveform and sound pressure waveform pairs for three holds: DBP (black), MAP (red), and sSBP (blue). Top row shows the characteristic pulse pressure waveforms, and the bottom row shows the extracted sound pressure waveforms. Each column represents a distinct individual from the clinical study.

These findings indicate that the WP1 oscillations from AES are present at all hold pressures but, at non-occlusive pressures, these oscillations are combined with local flow vibrations. These results confirm that the sound pressure waveform is independent of the hold pressure and the measured pressure oscillations are a property of the LV-AV coupling. Although, a direct representation of the sound pressure waveform free from local flow vibrations can be optimally obtained at the sSBP hold.

Validation of sound pressure waveform content with aortic catheter

An invasive catheter placed in the ascending AO is the method reported in the literature to measure the sound pressure waveform[7]. To validate the content of the cuff sound pressure waveform, we compared our methodology to sound pressure waveforms extracted from the catheter signal. For both the catheter and cuff, the digital filter discussed above was applied to the pressure time signals during the sSBP hold pressure segments to generate a simultaneous sequence of sound pressure waveforms. Figure 5A shows the sound pressure waveforms extracted from simultaneous cuff and catheter recordings in a subject from the study population. Both signals display a first pressure oscillation after the foot of the cardiac waveform, close to the beginning of systole, and second subsequent pressure oscillation, followed by a large interval of steady signal. A time delay is observed between the catheter and cuff sound pressure waveforms corresponding to the time delay of wave propagation in the cardiovascular system from central to brachial artery.

The time interval from WP1 to WP2 peaks was compared between the cuff and catheter sound pressure waveforms. The WP1 to WP2 peak time interval between catheter and cuff exhibited a strong measurement agreement (ICC = 0.69 [0.58, 0.78]) for the entire population (n = 106) (Fig. 5B). The average time delay measured between the catheter and cuff sound pressure waveform signal was of 58 ± 16 ms (Fig. 5C). These values align with expected wave propagation speeds for a population with these demographics[31,32].

The IF analysis was applied to the cuff and catheter sound pressure signals and the mean IF values around the oscillatory peaks, WP1 and WP2, were extracted for each subject. The mean cuff IF values for the study population was of 16.4 (3.1) Hz for WP1 and 15.8 (2.8) Hz for WP2 (Fig. 5D). The mean catheter IF values for the study population was of 17.3 (3.1) Hz for WP1 and 18.0 (1.9) Hz for WP2 (Fig. 5E). WP1 and WP2

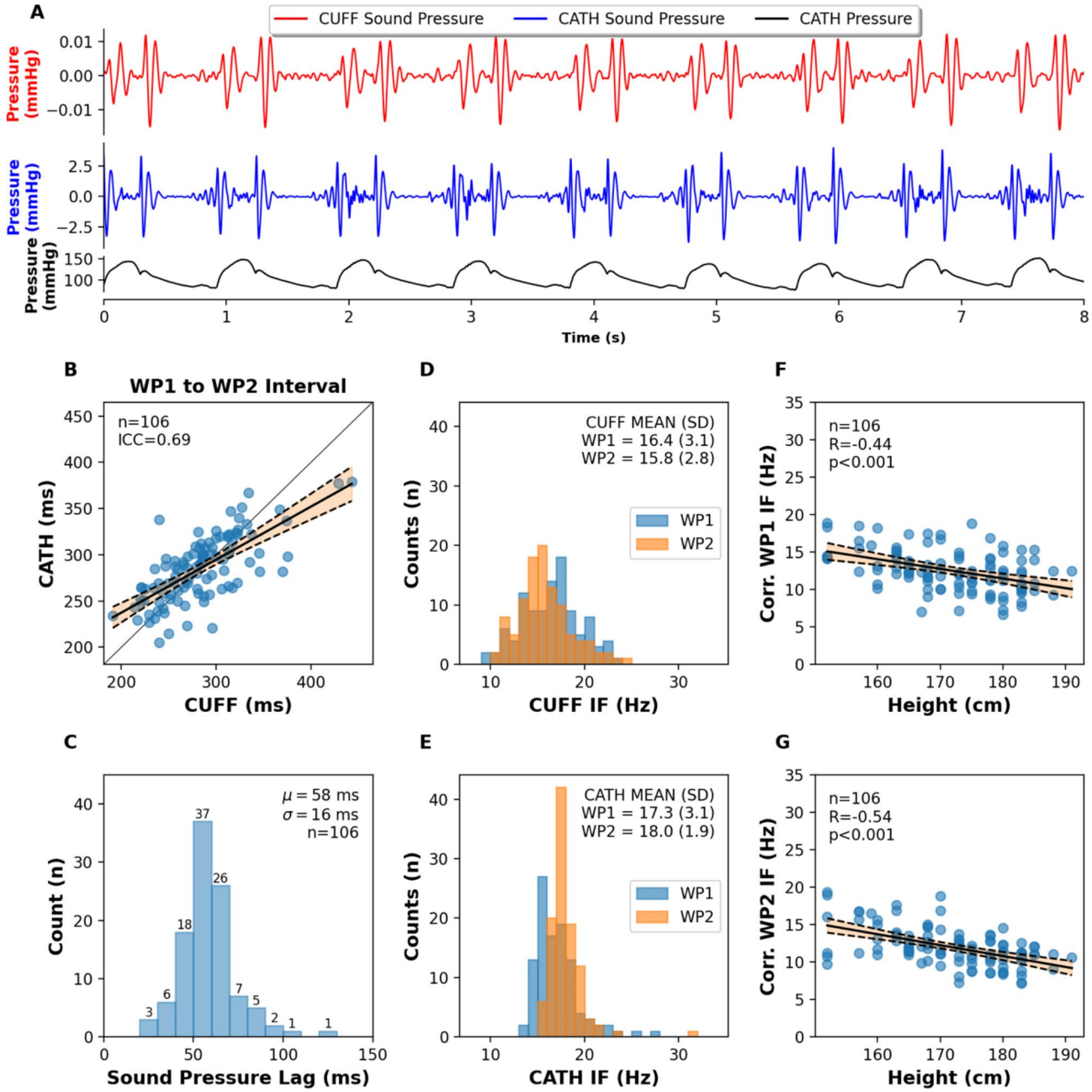

Fig. 5. Comparison between cuff and catheter sound pressure waveforms. (**A**) shows a simultaneous cuff (red line) and catheter (blue line) sound pressure waveform segment from a subject in clinical study. Catheter pressure signal (black) is provided as a timing reference. (**B**) scatter plot comparing the WP1 and WP2 peak time intervals between the cuff and catheter signals. (**C**) shows the average time delays of cuff sound pressure signal compared to catheter sound pressure signal. (**D**) and (**E**) show the Instantaneous Frequency analysis for the sound pressure signal WP1 and WP2 in the cuff and catheter, respectively. (**F**) and (**G**) show scatter plots for the correlation of the height with the corrected Instantaneous Frequency of the WP1 and WP2, respectively.

distributions closely overlapped for catheter and cuff measurements. The within subject differences on WP1 and WP2 for the cuff and catheter measurements are reported in Fig. S10. The mean IF frequencies for WP1 and WP2 were compared to physiological characteristics of subjects in the study population. Figure 5F and G show a moderate negative linear relationship between height and the corrected WP1 IF (Pearson-R = -0.44, $p < 0.001$) and a strong negative linear relation between height and the corrected WP2 IF (Pearson-R = -0.54, $p < 0.001$), respectively.

To rationalize the observed results, we model the cardiac structure transient vibrations using the mass-spring-damper subjected to external forcing by a Dirac delta function. In an underdamped system, the mass-spring-damper solution exhibits an exponentially decaying oscillatory behavior, with oscillatory frequency determined

by the damped natural frequency term. The damped natural frequency (f_d), in units of Hz, can be expressed in terms of mass (m), damping (c), and stiffness (k) as shown in Eq. (1),

$$f_d = \frac{1}{2\pi}\sqrt{\frac{k}{m} - \frac{c^2}{4m^2}} \tag{1}$$

For the cardiac system, the parameters of Eq. (1) can be related to physiological parameters. 'k' denotes the combined stiffness of the heart and aorta, approximated as $k \approx k_{aorta} + k_{heart}$. The stiffness of an elastic tube can be expressed as $k = Eh/r$, where E represents elasticity, r is the radius, and h is the wall thickness. 'm' represents the momentum mass, comprising the masses of the blood-filled aorta and heart, roughly $m \approx m_{aorta} + m_{heart}$. The mass of the blood-filled aorta is proportional to $L(\rho_{blood}A_{ID} + \rho_{wall}(A_{OD} - A_{ID}))$, where L is the segment length, ρ_{blood} is the density of blood, ρ_{wall} is the aortic wall density, A_{ID} is the aortic internal diameter, and A_{OD} is the aortic outer diameter. The mass of the heart can be simplified as, $m_{heart} \propto \rho_{heart}V_{heart}$, with ρ_{heart} representing heart density, and V_{heart} denoting heart volume. 'c' is the damping term which is challenging to directly relate with system properties.

This decomposition reveals that the damped natural frequency of the system correlates directly with its stiffness $\left(f_d \propto \sqrt{k}\right)$ and inversely with its dimensions, the diameter 'd', $\left(f_d \propto d^{-1}\right)$. Previous studies have established a relationship between height and aortic root diameter, allowing height to serve as a proxy for aortic diameter[33,34]. The findings in the literature align with this study's observed inverse relationship between height and IF. Interestingly, when extending the analysis to correlate age and weight as surrogate for stiffness, weak linear relationships were observed at best (Pearson-R < 0.25, p > 0.01) (Fig. S4). Additionally, regression analysis indicated no significant associations between height, age, or their interaction with WP1 and WP2 parameters, results are summarized in Table S2. This outcome is not surprising given this population has a high prevalence of cardiovascular conditions as reported in Table 1 and therefore the impact of age and weight on stiffness is secondary.

Sound pressure assessment of left ventricular contractility

Prior to the beat-to-beat analysis of LV contractility with cuff sound pressure waveform parameters, we evaluated the impact of the catheter placement through the AV on the measured signal. Subject-averaged comparison of the cuff sound pressure waveform parameters performed with the catheter in the LV and the AO recording showed good agreement for both morphology and features (Fig. S5) for: the WP1 to WP2 time interval (ICC = 0.87 [0.82, 0.91]), WP1 amplitude (ICC = 0.92 [0.88, 0.94]), and WP2 amplitude (ICC = 0.79 [0.71, 0.85]). These results confirm that the catheter in the LV, which passes through the AV, does not affect the sound pressure waveform signal as measured with the cuff, and therefore can be used for this beat-to-beat analysis.

The portion of the measurement with the catheter in the LV was analyzed to assess the correlation of cuff sound pressure waveform parameters to LV contractility. The LV contractility analysis utilizing the sound pressure waveform required a population free of heart valve disease. A pressure gradient analysis was implemented to measure the LV to AO pressure gradient and identify undiagnosed AV disease. The pressure gradient analysis successfully estimated the AV pressure gradient in all 106 individuals. The calculated pressure gradients ranged from − 19 to 35 mmHg; the negative pressure gradients are non-physiological and originate from methodology related limitations. Figure S6 summarized the results from the pressure gradient analysis.

Within the study population, 71 subjects passed all eligibility criteria for the LV contractility analysis. A total of 14 subjects were excluded for AV disease (9 reported from the patient questionnaire and 5 detected with the pressure gradient analysis) and 21 were excluded for lacking beat-to-beat segments longer than 5 sequential pulsations. This population subset (n = 71) was composed of 63% men with average age of 65 years. In the study population, 82% reported hypertension, 27% reported diabetes, and 72% reported hyperlipidemia. Table S1 summarizes the main characteristics of this population subset.

Simultaneous LV pressure and cuff sound pressure time sequences are used for pulse waveform analysis. Figure 6A shows an example of a five second time segment of LV pressure and cuff sound pressure waveforms. The simultaneous signals show that WP1 occurs after the LV pressure rise, upon opening of the AV, and WP2 develops with the LV pressure drop, upon closure of the AV. The LV isovolumetric contraction rate, dPdt-max, showed the highest positive linear correlation with the WP1 peak-to-peak amplitude corrected with a surrogate of arterial elasticity (Pearson-R = 0.65, p < 0.001) (Fig. 6B). The LV isovolumetric relaxation rate, ndPdt-max, showed the highest positive linear correlation with the WP2 peak-to-peak amplitude corrected for a surrogate of arterial elasticity (Pearson-R = 0.55, p < 0.001) (Fig. 6C). Correction for arterial elasticity was performed using wave propagation time from central to peripheral arteries; Fig. S7 shows the correlation between subject age and wave propagation time. The correlations for the full WP1 and WP2 parameter set, and LV contractility parameters are shown in Fig. S8 in the form of a correlation matrix. As reported in Fig. 6D, the measure of pressure wave intensity, p_{rms}, showed good correlation between the LV pressure wave and the cuff sound pressure wave (Pearson-R = 0.73, p < 0.001). The moderate yet statistically significant (p < 0.001) correlation observed between WP1 and ndPdt-max, as well as WP2 and dPdt-max, arises from the physiological interdependence in LV contractile functions. Despite being distinct mechanisms, they are inherently connected within the same physical structure. The results presented above show that the sound pressure waveform method is capable of non-invasively measuring the LV-AV coupling which directly correlates with LV contractility.

Regression analysis was performed to adjust the dPdt-max and ndPdt-max models for age, gender, systolic blood pressure (SBP), and heart rate (HR). The dPdt-max model explained 52.4% of the variance ($R^2 = 0.524$), with the WP1 parameter providing the largest contribution to the model (β = 176.54, p < 0.001). Additionally, SBP (β = 67.87, p = 0.022) and HR (β = 79.54, p = 0.009) were significant predictors. The model did not report

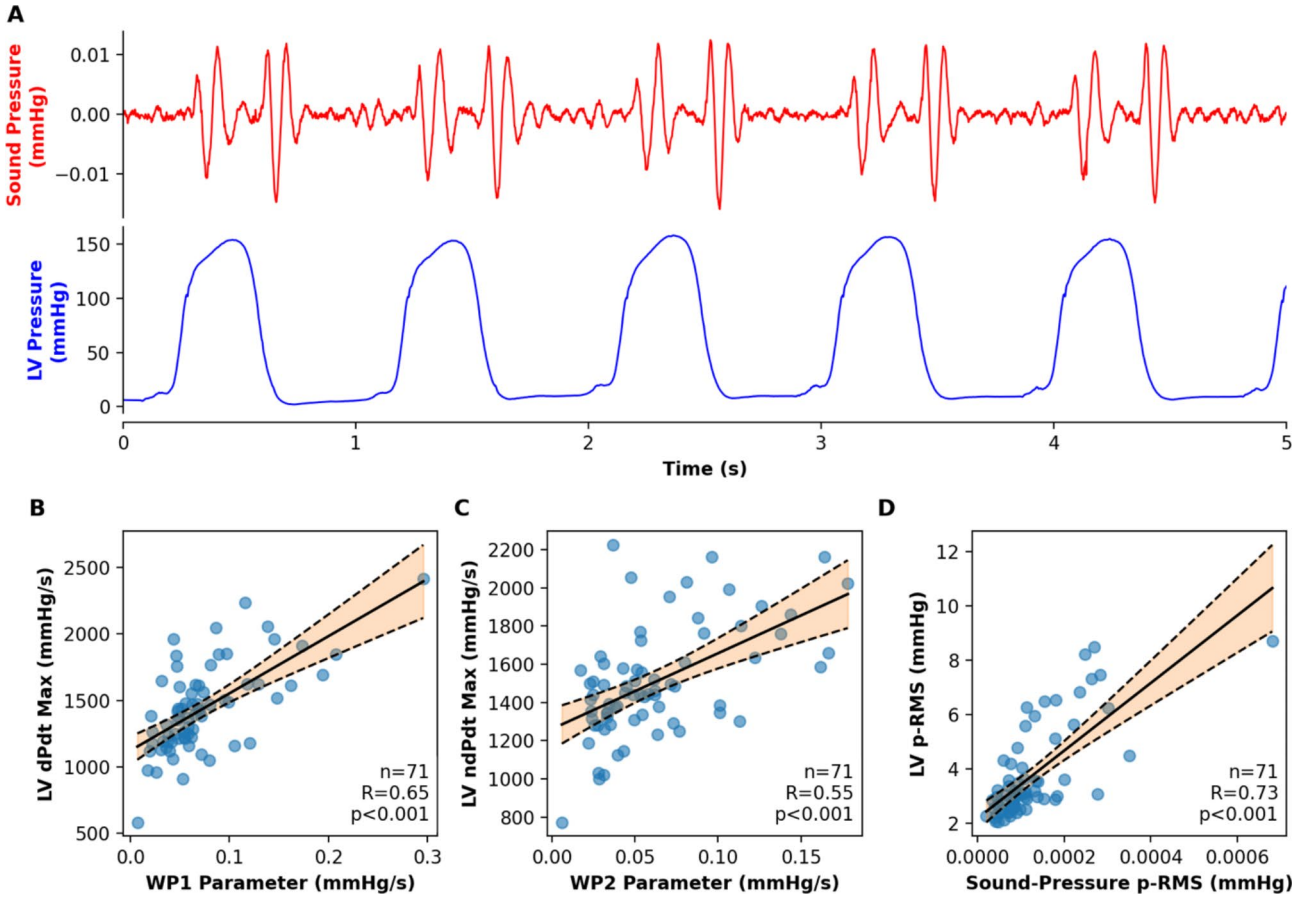

Fig. 6. Correlation of Left Ventricular (LV) contractility with cuff-based sound pressure waveform parameters. (**A**) shows a segment of the simultaneous cardiac signals analyzed inclusive of the cuff-based sound pressure waveform (red) and the invasive catheter LV pressure (blue). (**B**) shows the scatter plots of the LV dPdt-max versus the WP1 parameter. (**C**) shows the scatter plot of the LV ndPdt-max versus the WP2 parameter. (**D**) shows the scatter plot of the LV p-RMS versus the cuff sound-pressure p-RMS.

heteroskedasticity or non-normality of residuals. The ndPdt-max model explained 47.6% of the variance ($R^2 = 0.476$), with the WP2 parameter providing the largest contribution ($\beta = 157.75$, $p < 0.001$); gender ($\beta = -73.17$, $p = 0.008$) and heart rate ($\beta = 79.21$, $p = 0.003$) were also significant contributors. The Breusch-Pagan test statistic ($p < 0.001$) confirmed the presence of heteroskedasticity. Applying transformations to the dependent variable (square root, logarithmic, and Box-Cox) did not eliminate the heteroskedasticity. Model results are summarized in Tables S3 and S4 and Fig. S11.

Discussion

In this study, we present the clinical implementation of a cuff-based technique aimed at extracting and analyzing cardiac structure vibrations, commonly referred to as heart sounds, for non-invasive assessment purposes. By comparing our signal to invasive catheter measurements, which have been validated in the literature for this purpose, we demonstrated the ability to non-invasively capture pressure vibrations of the heart-aorta complex caused by the rapid acceleration and deceleration of blood flow at the onset and conclusion of systole, respectively[7,10,11]. Importantly, we have observed that the characteristics of these pressure vibrations are contingent upon the functional and geometric properties of the left side of the heart. Therefore, this methodology provides a robust platform for non-invasively interrogating the LV and AO.

Previous studies have suggested the presence of both low and high frequency oscillatory components within heart sounds. While low frequencies are embedded within the cardiac waveform and require a high-resolution system for detection, high frequencies propagate through the chest wall and are discernible with a stethoscope[9]. Technological advancements in signal resolution for brachial cuff devices have enabled the capture and separation of these lower frequency pressure vibrations embedded within the pulse pressure waveform[26]. Our concurrent application of cuff and stethoscope on healthy individuals has confirmed that these two systems capture distinct components of the cardiac system vibrations. Notable, while the stethoscope is typically utilized for diagnosing heart valve diseases, our study primarily focused on pressure related dynamic contractile behaviors. This distinction emphasizes that the cuff sound pressure technique measures a different pressure component and does not replace stethoscope measurements. Importantly, from an implementation standpoint, extracting

the sound pressure waveform from the cuff signal is a signal processing task. Since brachial cuffs are already commonly used in clinical practice, incorporating this approach into clinical practice would impose minimal additional burden. In contrast, using a conventional stethoscope requires a separate procedure and the expertise of a trained clinician. Moreover, the placement of the stethoscope on the chest significantly influences the capture signal, while our approach is relatively insensitive to cuff placement on the subject's arm[35]. Therefore, we assert that this cuff technique and the stethoscope should be viewed as complementary tool for a comprehensive heart sound assessment, rather than substitutes.

Given the rising incidence of left-sided heart failure, there is a pressing need for rapid assessment of LV function. The presented clinical data, with simultaneous catheter and brachial cuff recordings, highlights the potential of the sound pressure waveform from the cuff system as a non-invasive indicator of LV contractility, assessed via dPdt-max and ndPdt-max. The observed correlations followed the expected physiological outcome: increasing contractile strength of the LV will generate large amplitude pressure vibrations within the system. The integration of physiological understanding and the statistical outcomes obtained from this clinical evaluation establishes the basis for a cuff-based diagnostic tool to assess LV contractility. Regardless of the strength of these findings, it is important to consider the role of such measurements in current clinical procedures. Historically, the cuff has served as a first-line diagnostic tool, providing generalized cardiovascular risk assessment. Similarly, we envision that technological advances, such as those proposed herein, will generate more specific risk factors and will be utilized by healthcare professionals as additional guidance in determining the necessity for more advanced diagnostic procedures, such as echocardiography or catheterization. Leveraging the non-invasive, rapid, repeatable, and cost-effective nature of cuff measurements fulfills the ideal specifications and roles of an initial screening. Ultimately, providing condition specific risk factor can enhance accessibility to testing while reducing the burden on patients and the healthcare system.

Our analysis also aimed to explore the frequency component of the underlying mechanisms of cardiac structure pressure vibrations. As outlined in the literature, these vibrations stem from rapid changes in fluid momentum within the cardiohemic system, representing energy conversions between potential and kinetic states[7,10,11]. The structural and material properties of the system, analogous to a mass-spring-damper model, significantly influence the characteristics of these vibrations. While our findings indicated a moderate relationship between system dimensions and damped natural frequency, their clinical relevance lies in the potential to detect cardiovascular conditions affecting the structural properties of the heart and aorta. For instance, thoracic aortic aneurysms, characterized by weakened and widened aortic walls, are known to alter local pressure and flow dynamics[36–38]. Rabkin et al. found a direct correlation between the size of ascending thoracic aortic aneurysms and local aortic compliance. This correlation was observed in subjects who were already diagnosed with the condition and measured using carotid-to-femoral PWV[39]. Therefore, monitoring, and possibly detection, of such conditions, which are typically asymptomatic, could benefit from analysis of the sound pressure waveform as aneurysms are expected to induce significant structural modifications that translate to an oscillatory frequency change in the system. These insights serve as motivation for further research into the diagnostic applications of cardiac structure pressure vibrations from cuff devices, particularly in detecting silent cardiovascular conditions.

While our study offers valuable insights into the relationship between the cuff sound pressure waveform and cardiac structure vibrations, it is essential to address certain limitations and improvements. Firstly, the study population is not representative of the general population, as subjects were referred for left heart cardiac catheterization, resulting in a higher prevalence of cardiovascular conditions. Secondly, the limited population size did not allow for stratification based on parameters that are known to generate marked effects, such as age and gender. Additionally, our exclusion criteria, based on self-reported data and pressure gradient measurements, may not have entirely removed subjects with AV disease. The presence of negative pressure gradients in a significant portion of the data suggests potential disturbances that may have obscured individuals with undiagnosed AV disease.

Conclusion

The widespread and well-accepted brachial cuff as a diagnostic device allows for a direct implementation of the sound pressure waveform analysis without modifications of current clinical protocols. The non-invasive and repeatable nature of data collection with a brachial cuff enables healthcare professionals to effectively monitor disease progression and therapy effectiveness both in the clinic and at home. The availability of this additional clinical information does not impose any additional burden on clinical practitioners, as BP measurements using cuff systems are routinely conducted in clinics. Bridging the information gap between non-invasive diagnostic tools and their invasive counterparts represents a crucial stride towards achieving true personalized medicine.

Methods

Study data

The manuscript includes an invasive study and a non-invasive healthy control study. Both studies used the brachial cuff device described in the methods section; the brachial cuff measurement structure was the same for both studies and is described in the respective section.

The invasive study was approved by the Institutional Review Board (IRB) of the testing centers. All study participants provided formal written informed consent. The study was conducted in accordance with the principles outlined in the Declaration of Helsinki. This data included simultaneous pulse waveform acquisition with cardiac catheterization and brachial cuff. The catheter was first placed in the LV and then retracted to the ascending AO; a full cuff measurement was performed at each location.

The non-invasive healthy control study was approved by the Caltech IRB. All study participants provided formal written informed consent. Work adheres to the Declaration of Helsinki. The data included simultaneous

brachial cuff measurement and cardiac auscultation with a digital stethoscope. A full cuff measurement was performed while the stethoscope was in chest position 'A'.

Study population

The invasive study recruited individuals in a hospital setting between September 2021 and September 2022. The main inclusion criteria include age ≥ 21 years at the time of informed consent, referral for non-emergent left heart catheterization to be performed from either a femoral or radial access site, ability to participate in all study evaluations, allow access to medical records, and ability to understand and sign informed medical consent. The main exclusion criteria were experiencing a severe cardiac event within a week prior to the scheduled catheterization, obstruction or open wound causing inability to obtain a brachial BP measurement, and contraindication to cardiac catheterization by judgement of the interventional cardiologist.

The non-invasive study recruited individuals within the Caltech community during March 2024. The main inclusion criteria for the study included individuals age ≥ 21 years at the time of informed consent and ability to participate in all study evaluations. The main exclusion criterion was the presence of any known cardiovascular health condition.

Brachial cuff device description

Non-invasive brachial pulse waveform acquisition was performed with the cuff-based device developed and validated by Tamborini and Gharib[26,40]. The device consists of a non-invasive BP module with tourniquet capabilities and a pneumatic circuit for high-fidelity pulse waveform acquisition. The device was configured to perform a BP measurement followed by three instances of inflate-and-hold. For this study, the inflate-and-hold pressures were sequentially configured to DBP, MAP, and sSBP (SBP + 35 mmHg) for 30, 20 and 40 s, respectively. The device's data rate is of 1 kHz.

Method for extraction of heart sounds from brachial cuff

Cardiac auscultation through the brachial cuff-device relies on a digital filtering approach to isolate the sound pressure frequency content within the pulse pressure waveform. The digital filter was designed to capture the critical frequencies around which the cardiovascular sound pressures are generated[41]. The digital filter is applied using a forward filtering methodology to the pressure time signals captured with the cuff inflate and hold.

Optimal filter specifications to extract the sound pressure waveform from the brachial cuff were evaluated. The investigated aspects include filter type and filter cutoff frequencies. The filter type evaluated the frequency response of the filter, Gain and Phase, in the region of interest; this analysis included filter types of Butterworth, Elliptic, and Chebyshev Type 1, and Chebyshev Type 2. Filter type was evaluated for sharp transition phase and low phase distortion in the passband. The filter cutoff frequency explored the high-pass filter threshold around the reported heart sound range; this condition evaluated cutoff frequencies at 16, 18, 20, and 22 Hz. Optimal filter cutoff was assessed on the separation between the two expected sound pressure peaks.

Signal comparison with stethoscope

Simultaneous cuff and stethoscope measurements were performed to evaluate the equivalence of the content of these two signals. The study utilized the Cardionics E-Scope Electronic Stethoscope II to record heart sounds via analog output to the AD instruments data acquisition system. Subjects were placed in supine position with cuff on the left arm and the stethoscope in chest position A. Cardiac auscultation area A, which is between the second right intercostal space close to the upper sternal border, is optimal for auscultation of the AV. A full cuff measurement was performed. The cuff signal in the sSBP hold was analyzed to extract the sound pressure waveform with the method described herein. The signals from the two devices were analyzed to measure the timing indices of the wave peaks. Timing delays between the stethoscope and cuff peaks were evaluated in milliseconds on a beat-to-beat basis. The instantaneous frequencies of the stethoscope and cuff sound pressure signals were extracted using the Hilbert Transform for the analytical signal. The average IF in correspondence to the WP1 and WP2 peaks were extracted for comparisons.

Effect of cuff hold pressure on sound pressure waveform morphology

The effect of the hold pressure on the morphology of the sound pressure waveform was evaluated at three pressure holds – DBP, MAP, and sSBP – for subjects in the invasive study. For each subject, the sound pressure waveform filtering method was applied to the hold pressure signal. Then, the mean sound pressure waveform for the hold was generated by aligning the individual cardiac cycles and performing a time-based averaging. The average sound pressure waveform shapes from the holds were qualitatively compared.

Validation of sound pressure waveform content with aortic catheter

This analysis was performed on subjects in the invasive study. The cuff-based sound pressure waveform was compared with the sound pressure waveform extracted from the catheter in the ascending AO. Both catheter and cuff signals were processed during the sSBP hold portion of the measurement to extract simultaneous sound pressure waveforms. Each pressure signal was digitally filtered to extract the sound pressure waveform. The envelope function of the sound pressure waveform was analyzed to measure the WP1 and WP2 peak time intervals in the two signals. For each subject, the average time delay between the catheter and cuff sound pressure signals was measured as the average of the individual waveform cross-correlation lag. The IF analysis using the Hilbert Transform was applied to the cuff and catheter sound pressure waveforms. IF frequencies for the WP1 and WP2 peaks were extracted for each waveform and averaged across individuals for cuff and catheter signals. WP1 and WP2 IF were compared with patient characteristics from the medical questionnaire. IF correction was

performed using the square root of the ratio of the systolic to diastolic duration for the cardiac cycle as measured on the cuff waveform, $IF_{corr} = IF * \sqrt{\frac{T_{sys}}{T_{dia}}}$.

Sound pressure assessment of left ventricular contractility

This analysis used the invasive data. The clinical data was analyzed to detect a correlation between the sound pressure waveform and the LV contractility. The analysis required a population free of heart valve disease. Subjects were excluded from the study if they reported heart valve disease on the AV. Subjects with undiagnosed heart valve disease on the AV were identified using the transvalvular pressure gradient. A pressure gradient between the LV and the AO greater than 10 mmHg was used as the cutoff[42]. Subjects were also excluded if the recording failed to have a consecutive segment of at least 5 pulsations.

The portion of the measurement with the catheter in the LV during the sSBP pressure hold was used for this analysis. The cuff pressure signal was digitally filter with the specifications described above to extract the sound pressure waveform. Beat-to-beat pulse waveform analysis was performed on both catheter and cuff signals. Pulse waveform analysis on the LV waveforms measured contractility parameters inclusive of maximum isovolumetric contraction rate, dPdt-max, and maximum isovolumetric relaxation rate, ndPdt-max[43]. Pulse waveform analysis on the sSBP sound pressure waveform measured the amplitude, frequency, and envelope function slopes for the WP1 and WP2 pressure oscillations. Calibration and scaling methodologies were also applied to convert the amplitude parameters to physiological units. Calibration involved translating waveform amplitude by normalizing the sound pressure waveform with the average sSBP amplitude and then multiplying by pulse pressure magnitude. Scaling involved translating waveform amplitude by multiplying the normalized waveform by the instantaneous pressure value; for WP1 this is the waveform starting pressure and for WP2 this is the dicrotic notch pressure. Adjustment for arterial stiffness on the amplitude parameter was performed by using the wave propagation time as a surrogate for arterial elasticity. Wave intensity was assessed using the magnitude, measured as root-mean-square value, of the Fourier spectrum of the pressure time signals in the target range[44]. The catheter LV signal was analyzed in the 0–20 Hz range and the cuff sound pressure signal was analyzed in the 0–60 Hz range; Fig. S9 shows an example of the measured of pressure time signal wave intensity for the LV catheter and cuff sound pressure.

Statistical analysis

Statistical analyses were performed on the subject-averaged parameter values. The strength of the linear association between variables was evaluated using the Pearson correlation coefficient (Pearson-R). Measurement agreement between modalities or measurement locations was assessed using the intraclass correlation coefficient (ICC), with 95% confidence intervals also reported. R^2, the coefficient of determination, was used to measure the proportion of variance in the dependent variable explained by the independent variables. The Shapiro–Wilk test was conducted to assess the normality of residuals, while the Breusch-Pagan test was used to evaluate heteroskedasticity. Statistical significance was set at $\alpha < 0.05$. All analyses were performed using Python 3.11.

Data availability

All data generated or analyzed during this study are included in the published article.

Received: 29 May 2024; Accepted: 31 October 2024
Published online: 05 November 2024

References

1. Sacks, M. S. & Yoganathan, A. P. Heart valve function: A biomechanical perspective. *Philos. Trans. R. Soc. B Biol. Sci.* **362**, 1369–1391 (2007).
2. Lombard, J. T. & Selzer, A. Valvular aortic stenosis. *Ann. Intern. Med.* **106**, 292–298 (1987).
3. Tavel, M. E. Cardiac auscultation. *Circulation* **93**, 1250–1253 (1996).
4. Monge Garcia, M. I. et al. Performance comparison of ventricular and arterial dP/dtmax for assessing left ventricular systolic function during different experimental loading and contractile conditions. *Crit. Care* **22**, 325 (2018).
5. Roger, V. L. Epidemiology of heart failure. *Circ. Res.* **128**, 1421–1434 (2021).
6. Aghilinejad, A., Tamborini, A. & Gharib, M. A new methodology for determining the central pressure waveform from peripheral measurement using Fourier-based machine learning. *Artif. Intell. Med.* 102918 (2024).
7. Whittaker, A. V., Shaver, J. A., Gray, S. & Leonard, J. J. Sound-pressure correlates of the aortic ejection sound. *Circulation* **39**, 475–486 (1969).
8. Waider, W. & Craige, E. First heart sound and ejection sounds: Echocardiographic and phonocardiographic correlation with valvular events. *Am. J. Cardiol.* **35**, 346–356 (1975).
9. Piemme, T. E., Barnett, G. O. & Dexter, L. Relationship of heart sounds to acceleration of blood flow. *Circ. Res.* **18**, 303–315 (1966).
10. Sabbah, H. N. & Stein, P. D. Investigation of the theory and mechanism of the origin of the second heart sound. *Circ. Res.* **39**, 874–882 (1976).
11. Stein, P. D. & Sabbah, H. N. Origin of the second heart sound: Clinical relevance of new observations. *Am. J. Cardiol.* **41**, 108–110 (1978).
12. Sabbah, H. N. & Stein, P. D. Relation of the second sound to diastolic vibration of the closed aortic valve. *Am. J. Physiol. Heart Circ. Physiol.* **234**, H696–H700 (1978).
13. Sikarskie, D. L., Stein, P. D. & Vable, M. A mathematical model of aortic valve vibration. *J. Biomech.* **17**, 831–837 (1984).
14. Kupari, M. Aortic valve closure and cardiac vibrations in the genesis of the second heart sound. *Am. J. Cardiol.* **52**, 152–154 (1983).
15. Luisada, A. A. & Portaluppi, F. The main heart sounds as vibrations of the cardiohemic system: Old controversy and new facts. *Am. J. Cardiol.* **52**, 1133–1136 (1983).
16. Sakamoto, T., Kusukawa, R., Maccanon, D. M., Luisada, A. A. & Harvey, I. Hemodynamic determinants of the amplitude of the first heart sound. *Circ. Res.* **16**, 45–57 (1965).
17. Kusukawa, R., Bruce, D. W., Sakamoto, T., MacCanon, D. M. & Luisada, A. A. Hemodynamic determinants of the amplitude of the second heart sound. *J. Appl. Physiol.* **21**, 938–946 (1966).

18. Stein, P. D., Sabbah, H. N. & Barr, I. Intensity of heart sounds in the evaluation of patients following myocardial infarction. *Chest* **75**, 679–684 (1979).
19. Raff, G. L. & Glantz, S. A. Volume loading slows left ventricular isovolumic relaxation rate. Evidence of load-dependent relaxation in the intact dog heart. *Circ. Res.* **48**, 813–824 (1981).
20. Frederiksen, J. W., Weiss, J. L. & Weisfeldt, M. L. Time constant of isovolumic pressure fall: Determinants in the working left ventricle. *Am. J. Physiol. Heart Circ. Physiol.* **235**, H701–H706 (1978).
21. Kumada, T. et al. Usefulness of negative dP dt upstroke pattern for assessment of left ventricular relaxation in coronary artery disease. *Am. J. Cardiol.* **63**, E60–E64 (1989).
22. Sabbah, H. N., Khaja, F., Anbe, D. T., Folger, G. M. & Stein, P. D. Determinants of the amplitude of the aortic component of the second heart sound in aortic stenosis. *Am. J. Cardiol.* **41**, 830–835 (1978).
23. Stein, P. D., Sabbah, H. N., Khaja, F. & Anbe, D. T. Exploration of the cause of the low intensity aortic component of the second sound in nonhypotensive patients with poor ventricular performance. *Circulation* **57**, 590–593 (1978).
24. Sabbah, H. N., Khaja, F., Anbe, D. T. & Stein, P. D. The aortic closure sound in pure aortic insufficiency. *Circulation* **56**, 859–863 (1977).
25. Shindler, D. M. Practical cardiac auscultation. *Crit. Care Nurs. Q.* **30**, 166–180 (2007).
26. Tamborini, A. & Gharib, M. A pneumatic low-pass filter for high-fidelity cuff-based pulse waveform acquisition. *Ann. Biomed. Eng.* **51**, 2617–2628 (2023).
27. Baicu, C. F., Zile, M. R., Aurigemma, G. P. & Gaasch, W. H. Left ventricular systolic performance, function, and contractility in patients with diastolic heart failure. *Circulation* **111**, 2306–2312 (2005).
28. Meno, F., Reddy, P. S. & Bernardi, L. Heart sound propagation in the human thorax. *Clin. Phys. Physiol. Meas.* **6**, 123 (1985).
29. Voin, V., Oskouian, R. J., Loukas, M. & Tubbs, R. S. Auscultation of the heart. *Clin. Anat.* **30**, 58–60 (2017).
30. Shevchenko, Y. L. & Tsitlik, J. E. 90th Anniversary of the development by Nikolai S. Korotkoff of the auscultatory method of measuring blood pressure. *Circulation* **94**, 116–118 (1996).
31. The Reference Values for Arterial Stiffness' Collaboration. Determinants of pulse wave velocity in healthy people and in the presence of cardiovascular risk factors: 'Establishing normal and reference values'. *Eur. Heart J.* **31**, 2338–2350 (2010).
32. Díaz, A., Galli, C., Tringler, M., Ramírez, A. & Cabrera Fischer, E. I. Reference values of pulse wave velocity in healthy people from an urban and rural Argentinean population. *Int. J. Hypertens.* **2014**, e653239 (2014).
33. Svensson, L. G., Kim, K.-H., Lytle, B. W. & Cosgrove, D. M. Relationship of aortic cross-sectional area to height ratio and the risk of aortic dissection in patients with bicuspid aortic valves. *J. Thorac. Cardiovasc. Surg.* **126**, 892–893 (2003).
34. Davis, A. E. et al. Observational study of regional aortic size referenced to body size: Production of a cardiovascular magnetic resonance nomogram. *J. Cardiovasc. Mag. Resonance* **16**, 9 (2014).
35. Kawamura, Y., Yokota, Y. & Nogata, F. Propagation route estimation of heart sound through simultaneous multi-site recording on the chest wall. In *Annu Int Conf IEEE Eng Med Biol Soc* Vol. 2007 2875–2878 (2007).
36. Jin, W. & Alastruey, J. Arterial pulse wave propagation across stenoses and aneurysms: Assessment of one-dimensional simulations against three-dimensional simulations and in vitro measurements. *J. R. Soc. Interface* **18**, 20200881 (2021).
37. Nawrocka, I. et al. Abdominal aortic aneurysm influences the indices of arterial stiffness recorded by pulse wave analysis. *Arter. Hypertens.* **27**, 99–106 (2023).
38. Swillens, A. et al. Effect of an abdominal aortic aneurysm on wave reflection in the aorta. *IEEE Trans. Biomed. Eng.* **55**, 1602–1611 (2008).
39. Rabkin, S. W., Chan, K. K., Chow, B. & Janusz, M. T. Pulse wave velocity involving proximal portions of the aorta correlates with the degree of aortic dilatation at the sinuses of valsalva in ascending thoracic aortic aneurysms. *Ann. Vasc. Dis.* **7**, 404–409 (2014).
40. Tamborini, A. & Gharib, M. Validation of a suprasystolic cuff system for static and dynamic representation of the central pressure waveform. *J. Am. Heart Assoc.* e033290.
41. Stein, P. D., Sabbah, H. N., Lakier, J. B., Magilligan, D. J. & Goldstein, D. Frequency of the first heart sound in the assessment of stiffening of mitral bioprosthetic valves. *Circulation* **63**, 200–203 (1981).
42. Nishimura, R. A. & Carabello, B. A. Hemodynamics in the cardiac catheterization laboratory of the 21st century. *Circulation* **125**, 2138–2150 (2012).
43. Gleason, W. L. & Braunwald, E. Studies on the first derivative of the ventricular pressure pulse in man. *J. Clin. Invest.* **41**, 80–91 (1962).
44. Sabbah, H. N. & Stein, P. D. Turbulent blood flow in humans: Its primary role in the production of ejection murmurs. *Circ. Res.* **38**, 513–525 (1976).

Author contributions

A.T. and M.G. conceptualized the study, developed the methodology, and conducted the investigation. A.T. performed the data analysis, wrote the original draft, and reviewed and edited the manuscript. M.G. was responsible for funding, project supervision, and reviewed and edited the manuscript.

Funding

Cherng Fellowship from the Andrew and Peggy Cherng Department of Medical Engineering, California Institute of Technology; Gakenheimer Fellowship, California Institute of Technology.

Competing interests

The authors declare no competing interests.

Additional information

Supplementary Information The online version contains supplementary material available at https://doi.org/10.1038/s41598-024-78554-5.

Correspondence and requests for materials should be addressed to A.T.